Marine sediment contamination and dynamics at the mouth of a contaminated torrent: The case of the Gromolo Torrent (Sestri Levante, north-western Italy)

Marco Capello[1], Laura Cutroneo[1], Sirio Consani[1], Enrico Dinelli[2], Greta Vagge[1], Cristina Carbone[1]

1 DISTAV, University of Genoa, 26, Corso Europa, Genoa I-16132, Italy
2 BiGeA, University of Bologna, 1, Piazza di Porta San Donato, Bologna I-40126, Italy

In this study we have examined the currents and hydrological characteristics of the water column off the mouth of the Gromolo Torrent (north-western Italy) in relation to the grain-size, mineralogical characteristics and metal distribution in the marine sediment sampled. Our purpose was to quantify and map the contamination that was carried out to sea from the abandoned Libiola Fe-Cu sulphide mine that has heavily impacted the torrent. Our results show high concentrations of Cu and Zn, and relatively high concentrations of Cd and Ni inside the bay into which the Gromolo Torrent flows. However, high concentrations of As, Cr, Hg, Mn, Pb, and V found in the northern and/or eastern parts of the study area originated from other sources. The subdivision of study stations in terms of metal and mineral contents in the bottom sediments highlighted the clear influence of the currents on their dispersion and distribution in the area

Introduction

Human activities, such as mining, can cause high levels of contamination in the nearby coastal environment. In particular, the discharge from mining activity, such as mine drainage, characterised by high metal concentrations, represents a long-term source of metal contamination in rivers and torrents that can persist long after the end of the mining operations (da Silva et al., 2009).

The evidence of river and torrent contamination due to Acid Mine Drainage (AMD) is extensive and many researchers have focused on the different aspects of both geochemically- and biologically-related processes, studying the characteristics and behaviour of the contaminants in river environments (Edraki et al., 2005; Blowes et al., 2003; Matlock et al., 2002) and the impact of AMD on biological communities (Adlassnig et al., 2013; Baker et al., 2009; DeNicola and Stapleton, 2002; Gerhardt et al., 2004; Halter et al., 2012; Harding, 2005; Luís et al., 2009). Studies of the treatment and reclamation of AMD are also numerous (Akcil and Koldas, 2006; Johnson and Hallberg, 2005; Sheoran and Sheoran, 2006).

Due to the fact that rivers and torrents are major contributors to marine contamination, the impact of this input on the marine environment cannot be ignored (Nicolau et al., 2006). The processes that take place during the mixing of contaminated fresh waters and sea waters at river mouths and regulate the initial diffusion and dispersion of metals in the marine environment are complex and include dissolution, desorption, transformation and migration across the sediment/water interface (Asta et al., 2014). The physical-chemical parameters that mostly affect the metal diffusion in the marine system are salinity, pH, the water temperature, the properties of the sediments and the dynamics of the area (Duran et al., 2012; Nieto et al., 2007).

AMD from the Libiola Fe-Cu sulphide mine, located about 8 km NE of Sestri Levante (north-western Italy) and extended over an area of about 4 km^2 within the basin of the Gromolo Torrent, has contaminated the waters and sediments of the torrent (Carbone et al., 2005). The mine was extensively exploited from 1864 until 1962, with more than one million tonnes of minerals extracted, and then abandoned, but it still presents serious environmental problems due to various processes, such as supergenic sulphide oxidation, erosion of waste deposits, and easily accessible mine adits, which continuously discharge strong acid waters and, sometimes, toxic gases (Carbone et al., 2005).

In recent years, geochemical studies have been conducted on the chemistry of the water and particulate matter that leak from the mining area into the waters of the Gromolo Torrent (Dinelli et al., 2001; Dinelli and Tateo, 2002), the contamination rate of the torrent waters and sediments (Accornero et al., 2005; Carbone et al., 2013; Cortecci et al., 2008; Dinelli et al., 2001), and the impact of the mine waters on the biological sector (Cantonati et al., 2014). Up to now, no research has been carried out on the marine environment (neither sea waters nor sea sediments) off the torrent mouth to determine which contaminants have been transferred from the Gromolo Torrent to the sea and their distribution in the marine bottom sediments.

Therefore, the aim of this study is to determine the level of contamination of the marine bottom sediments off the mouth of the Gromolo Torrent ("Baia delle Favole" of Sestri Levante) and to identify the main sources and diffusion paths of the contaminants, considering the currents of the area, the mineralogy, and the sedimentary characteristics of the bottom sediments.

Study area

The coast and sea of Sestri Levante

The study area (Fig. 1) is situated between the mouth of the Entella Torrent (west) and the Punta Manara headland (east), and comprises the headland of Sestri Levante with two bays, the western named "Baia delle Favole" and the eastern named "Baia del Silenzio".

As reported by Doglioli et al. (2004a, b) the study area is characterised by the presence of a permanent north-westward current flowing roughly along the isobath and following the narrow shelf, with only short inversion time periods. The surface current intensity is generally of 25 cm s^{-1}, with a maximum of 100 cm s^{-1} during very strong winter winds. The bottom current velocity is 10 cm s^{-1}, with a winter maximum of 40 cm s^{-1}. A south-eastward gyre is generated by the presence of the headland (Doglioli et al., 2004a) and, moreover, an eastward counter-current is present along the north coast with a resulting drift of the coastal materials from the Entella Torrent to the Sestri Levante bay area (CNR and MURST, 1997).

The wave regime in the area is mainly determined by southern winds (SE, Scirocco, and SW, Libeccio), with the greatest storms caused by the autumnal south-western winds, with a maximum wave height of about 7 m.

The western bay of Sestri Levante (Baia delle Favole) is characterised by a shoreline extending for about 1300 m, interrupted by the mouth of the Gromolo Torrent: the northern section extends for 800 m from the NE to the SW, and the southern section for 500 m from the NW to the SE. The southern section extends to the headland with the breakwater of the marina of Sestri Levante (about 120 m-length).

As shown in Di Matteo and Milli (2008) the bathymetry of the bay is characterised by a gradual deepening of the bottom in the northern part of the study area and a shallower slope inside the bay off the Gromolo Torrent mouth, with the maximum depth of 14 m at the head of the marina breakwater.

The coast of the area consists mainly of sandstones with alluvial sediments around the mouth of the Gromolo Torrent (Dinelli et al., 2001).

The Gromolo Torrent

The Gromolo Torrent originates about 11 km from the coast of Sestri Levante (850 m a.s.l.), and has a catchment surface of 18.2 km^2, and a main sector length of 9 km oriented NE-SW. The catchment basin is characterised by a unimodal rain distribution with a maximum in November (thirty-year mean rain N180 mm) and minimum in July (Provincia di Genova, 2009). The corresponding flow rate of the torrent is at a minimum in July–August (minimum in the period 2010–2014 of −0.13 m with respect to the reference hydrometric level) and a maximum in October and November (maximum in the period 2010–2014 of 0.47 m with respect to the reference hydrometric level) (http://

Geologically, the catchment area of the Gromolo Torrent can be divided into three macro sectors: a north-eastern sector, which is characterised by a Jurassic ophiolithic sequence of serpentinites and basalts with their sedimentary cover, where the Libiola mine is located; a central sector that includes the central and lower parts of the Gromolo Torrent valley, where a turbidite sequence of sandstones and shales of an underwater cone crops out; and a south-western sector consisting of the flood plain of the final stretch of the torrent (Dinelli et al., 2001).

The Gromolo Torrent catchment area is characterised by woods in its upper reaches, woods alternating with cultivated areas in the valley bottom and terraced slopes, and the city of Sestri Levante and its hamlets close to the coast (about 19,000 inhabitants). The most important activity in the area is the shipyard of Riva Trigoso (Fig. 1) and smaller companies operating in the construction, paper and wood, engineering and textile sectors (Passarelli, 2001). Moreover, from 1905 to 1995 a metal factory producing pipes in iron, steel, copper and other metals (120,000 m^2 of maximum surface) operated along the torrent.

The Libiola Mine area (Fig. 1), located between 230 and 335 m a.s.l., is delimited by three tributaries of the Gromolo Torrent, and the mine waters flow into these creeks and directly into the Gromolo Torrent. The hydrological regime of the mining area is characterised by a constant outflow of water from the tunnels due to the presence of over 30 km of underground passages plus extensive open-cut mines that facilitate the drainage of rainwater. The main ore-forming minerals are pyrite, chalcopyrite and sphalerite, hosted in a quartz and/or calcite gangue. The water circulating in the mining area is mostly acidic sulphate water with a high percentage of dissolved Fe, Al, Cu, Zn, Ni, and other metals. A wide variety of secondary minerals precipitate from these solutions, mainly as colloids occurring in the AMD-impacted streams and runoff. These precipitates can scavenge high percentages of dissolved metals from solution and can subsequently act as a secondary source of contaminants through desorption or destabilisation processes. In particular, the Libiola mine colloidal precipitates can release Al, Cu, Fe, and Zn in solution, and, to a lower extent, Cd, Co, Mn, and Ni (Carbone et al., 2013; Consani et al., 2016). At two different sites along the Gromolo Torrent these acidic, metal-rich solutions (pH ≈ 2.6 and EC ≈ 6000 μS) are discharged directly into the alkaline water of the torrent, and the formation of an amorphous, metal-rich precipitate takes place (Accornero et al., 2005; Dinelli et al., 2001; Dinelli and Tateo, 2002; Marini et al., 2003). These colloids contribute to the dispersion of metals along the entire torrent course to its mouth and then into the sea.

Materials and methods

Instrumentations and sampling strategy

The distribution of the sampling stations was adapted to the characteristics of the area, with a higher concentration of stations in the western bay of Sestri Levante and more widely spaced stations westwards along the coast and off the bay (Fig. 2). A reference station (mentioned as "Bianco") was situated on the other side of the headland of Sestri Levante (in front of the eastern bay).

Superficial bottom sediments were sampled using a 5-L Van Veen grab. About 500 mL of sediment was collected at each station and stored in wide-necked plastic jars.

The hydrological data were collected using a conductivity–temperature–depth (CTD) multiparametric probe (IdromarAmbiente) equipped with a turbidimeter (Turner Designs), an optical sensor that determines the concentration of suspended particles in the water by measuring the incident light scattered at right angles, and expresses it in Formazin Turbidity Units (FTU). The Formazin is a polymer used to calibrate the sensor, and the sensor utilised in this study had a

Fig. 1. The study area of Sestri Levante, in north-western Italy, lies between the mouth of the Entella Torrent and Punta Manara; the Gromolo Torrent is indicated by a light blue line and the Libiola mine is indicated by a red circle (satellite imagery from Google Earth, Version 7.1.1.1888
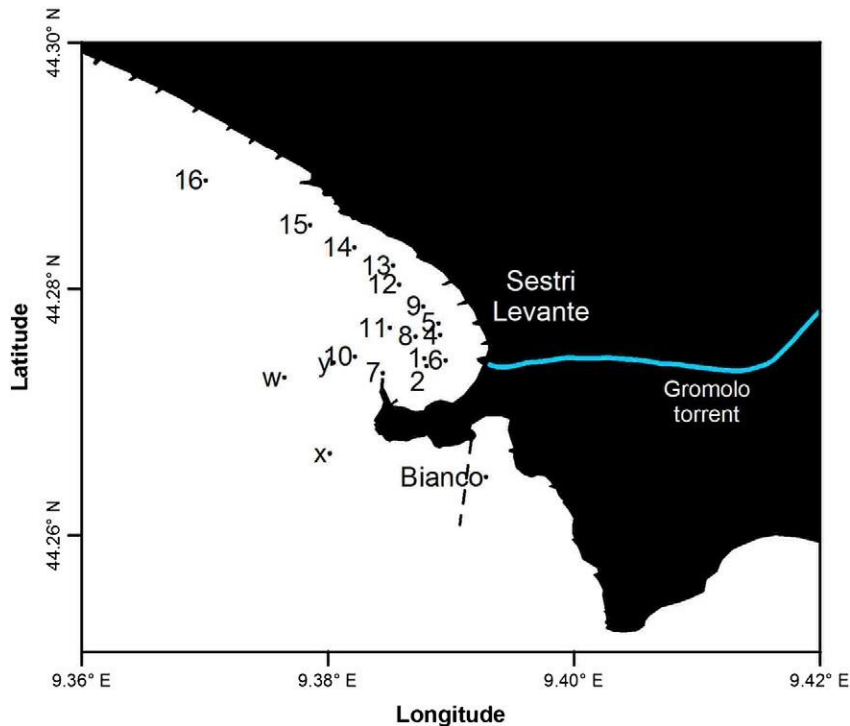
measurement range between 0 and 25 FTU. The salinity was determined using the Practical Salinity Scale.

A Teledyne RDI 600-kHz Workhorse® over-the-side-mounted current meter (Vertical Acoustic Doppler Current Profile - V-ADCP) with bottom-track function, using a 316L stainless-steel bracket, was used to collect the current velocity and direction data. RDI software "WinRiver® II" running on a notebook was used to collect and display the data in real time. Navigational data received from an external global

positioning system (GPS) were collected and used in the data postprocessing. The geographical coordinates and depth of the sampling stations are given in Table 1.

Table 1

Geographic coordinates of the study stations, samples and measurements carried out at each station.

Stations	Latitude (° N)	Longitude (° E)	Sea bottom depth (m)	Samples and measurements
1	44.2744	9.3878	5	Sediments
2	44.2738	9.3880	5	Sediments
4	44.2763	9.3891	7	Sediments
5	44.2772	9.3890	7	Sediments
6	44.2742	9.3896	6	Sediments, dynamics, hydrology
7	44.2732	9.3845	14	Sediments, dynamics, hydrology
8	44.2762	9.3871	9	Sediments, dynamics, hydrology
9	44.2786	9.3878	7	Sediments, dynamics, hydrology
10	44.2745	9.3822	14	Sediments, dynamics, hydrology
11	44.2769	9.3851	10	Sediments, dynamics, hydrology
12	44.2804	9.3858	7	Sediments, dynamics, hydrology
13	44.2819	9.3853	7	Sediments, dynamics, hydrology
14	44.2834	9.3822	7	Sediments, hydrology
15	44.2852	9.3786	7	Sediments, hydrology
16	44.2888	9.3701	9	Sediments, hydrology
Bianco	44.2647	9.3928	15	Sediments, dynamics, hydrology
w	44.2729	9.3765	20	Dynamics, hydrology
x	44.2667	9.3801	28	Dynamics, hydrology
y	44.2740	9.3805	15	Dynamics, hydrology

g. 2. Sample stations in the study area. The letters indicate the stations where only the dynamics and hydrological data were collected, while
e numbers correspond to the stations where the bottom sediments were also sampled. The light blue line indicates the Gromolo Torrent; the
ack dashes indicate the sewer outlet of the city of Sestri Levante (depth of the wastewater discharge: 35.5 m).

Laboratory analysis and data treatment

Sediment samples were homogenised and then divided into two portions for the intended analyses (grain-size distribution, mineralogical composition, and chemical content) and storage.

The grain-size analysis was obtained using wet sieving to divide the fine fraction (Ø b 63 μm) from the coarse one (Ø ≥ 63 μm), and then dry sieving to split the coarse fraction into the various sand and gravel granulometric classes (125, 250, 500, 1000 μm for sand, and Ø N 2000 μm for gravel). The results of grain-size distribution were expressed in % values.

Due to the fact that extensive precipitation of Fe(III)-bearing colloids takes place throughout the entire area of the mine in acidic water and as a result of the mixing of acid mine-waters with local streams and ground waters (Dinelli and Tateo, 2002; Grosbois et al., 2007; Kimball et al., 1995; Marescotti et al., 2008), and that metals tend to concentrate in particles of silt-clay size (Morillo et al., 2004; Villaescusa-Celaya et al., 2000), we only performed the chemical and mineralogical analyses on the two finest dimensional fractions of the marine sediment (Ø b 63 μm and $63 \leq \emptyset \leq 125$ μm fractions) derived from the sieving.

Therefore, after the grain-size separation, a portion of fine fraction (Ø ≤ 63 μm) and a portion of very fine sand ($63 \leq \emptyset \leq 125$ μm, hereafter called "coarse fraction") were analysed for the mineralogical characterisation using X-ray Powder Diffraction (XRD) analysis with CoKα radiation (current 20 mA, voltage 40 kV): the dry sediment portions were primarily ground with an agate mortar and pestle, and then mounted on zero-background silicon plates. After, each sample was scanned for 2θ (total scattering angle) between 5° and 80° at a scan rate of 5° min^{-1}.

The minerals of the samples analysed in the different XRD data were identified using the Powder Diffraction File™ (PDF) database of the International Centre for Diffraction Data (ICDD). Their quantification was performed using the Reference Intensity Ratio (RIR) method, which permits the mineralogical composition scaling of all diffraction data to the diffraction of standard reference materials.

The results of the mineralogical composition of the samples were expressed in % values.

Eleven metals and trace elements (As, Cd, Cr, Cu, Fe, Hg, Mn, Ni, Pb, V, and Zn), from the two sediment fractions studied (fine and coarse fractions) from each station, were determined and then considered in this work. Inductively Coupled Plasma Mass Spectrometry (ICP-MS) analysis was applied to 0.5 g of dry and ground sample after modified Aqua Regia digestion (ISO 15587), a method based on an acid mixture containing three volumes of concentrated hydrochloric acid and one of nitric acid used for the digestion of solid samples and the subsequent analysis of elements. The Aqua Regia digestion and ICP-MS analysis (AQ250 standard package) was performed by Bureau Veritas Mineral Laboratories (Canada; ISO9001 Quality Management Systems). Standard quality assurance procedures include: analysis of blanks within each batch; a routine testing of certified reference materialstandards; duplicate samples included in each batch to ensure that reproducible results are being achieved.

The distribution maps of the analytical results of the currents, hydrological characteristics, and sediment dimensions were drawn using the standard Kriging method of interpolation, while the distribution maps of the contaminant concentrations were drawn using the Classed Post Map; both methods were performed with Surfer® software (Golden Software Inc., ver. 10).

To define and discuss the relationship between the metals and mineralogical characteristics of the sediment samples, the Spearman's rank correlation was employed (Preda and Cox, 2002). In addition, principal component analysis (PCA) was used to simplify the interpretation of the grouping of the stations due to the metal distribution in the bottom sediments.

Results

Our sediment samples were principally characterised by coarse materials (Ø N 63 μm; Table 2), mostly consisting of fine sand, with values between 56 and 84% at all the sampling stations, with the exception of station 2, which had 36% fine sand and a prevalence of mean sand (42%). The highest value recorded for fine materials (Ø b 63 μm) was 17%, with an average of about 9% in the analysed samples.

The horizontal distribution of the fine (Ø b 63 μm) and coarse (Ø N 63 μm) sediments in the study area (Fig. 3) highlighted a general prevalence of the coarse materials, but in the bay the percentage of coarse sediment decreased (83% at stations 1 and 9) and, consequently, the fine sediment increased. On the contrary, outside the bay the coarse sediment percentages were higher, reaching a maximum of 95.8% at Bianco station.

In the offshore surface layer (Fig. 4), currents flowed from E to W following the general circulation of the Ligurian Sea (Millot and TaupierLetage, 2005), while inshore, a counter-current flowed from W to E, following the profile of the bay and the headland of Sestri Levante, producing a gyre inside the bay. The counter-current was also present in the

Table 2

Basic statistics for grain-size variations in the 16 sediment samples. Values are expressed in % of the total sample.

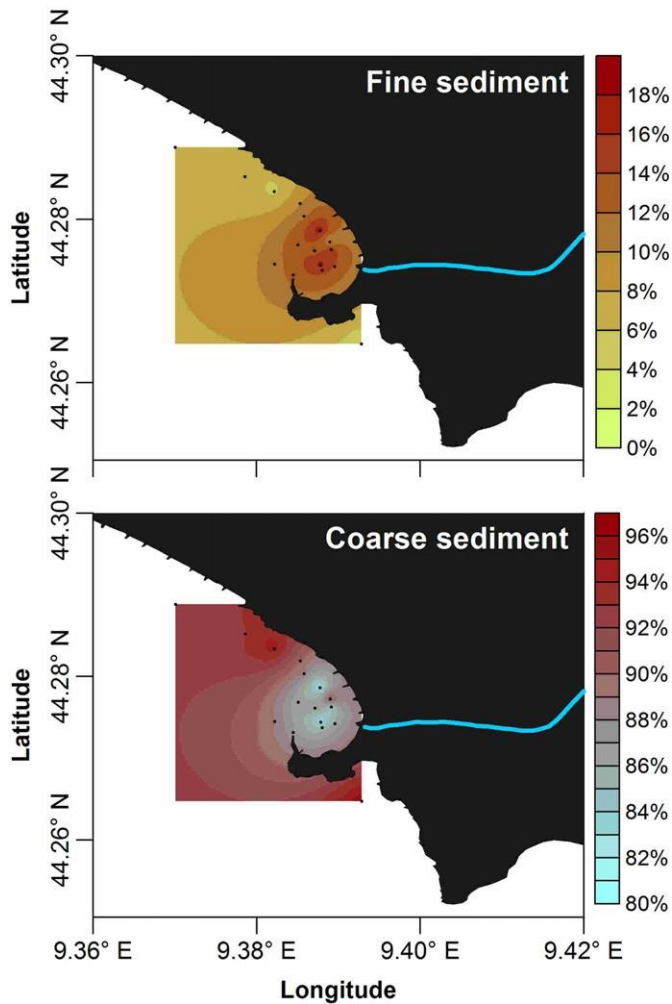|	Fine sediment (Ø b 63 μm)	Coarse sediment (Ø N 63 μm)	Very fine sand ($63 \leq \emptyset \leq$ 125 μm)	Fine sand (125 $\leq \emptyset \leq 250$ μm)
Minimum	3.9	82.8	6.8	36.0
Maximum	12.9	95.8	30.4	83.5
Mean	8.6	88.6	15.9	67.9
Median	9.3	88.0	15.4	71.2
Standard deviation	3.0	3.9	7.0	11.2

Fig. 3. Distribution of sediment fractions. The ranges of the classes are in %. We considered the coarse-sediment fraction as sand + gravel as the gravel fraction was negligible (only 0.1% of the whole sample.

bottom layer, flowing W-E, and was also followed by the offshore currents, which are, therefore, contrary to the general current trend of the Ligurian Sea. The current intensity was relatively low, above all inshore and inside the bay, and in general did not exceed 20 cm s^{-1}.

The salinity (Sal) of the water column (range 37.6–38.4; Fig. 5a) was lower in the bay and at Bianco station than off the headland of Sestri Levante and along the northern coast of the study area. The water temperature (T) (range 17.6–24.8 °C; Fig. 5b) had relatively lower values in the entire water column inside the bay and in the surface layer off the headland than in the northern part of the area. In the bottom layer of the northern part, the water temperature was affected by surface warming inshore where the depths are shallow, and showed a gradual decrease towards the open sea with the deepening of the sea bottom. The

water turbidity (Tu) (0.6–3.3 FTU; Fig. 5c) was low in the entire study area and was lower in the surface layer than in the bottom layer. In particular, turbidity was lower in the surface layer inside the bay (with the exception of station 6) than offshore, while it was the contrary in the bottom layer.

The concentration ranges for each contaminant found in the two considered sediment fractions (Ø b 63 μm and 63 ≤ Ø ≤ 125 μm) are reported in Table 3. Contaminant concentrations found were compared to values adopted in the national regulatory guidelines legislation for monitoring Italian coastal marine areas (D.M. 367/03; Table 3). In the fine fraction (Ø b 63 μm), the Cr and Ni concentrations were always higher than the legal limit, while As and Pb exceeded it only in some samples. Hg was always lower than the limit but, the maximum concentration was very close to it (285.0 ppb). In the coarse fraction (63 ≤ Ø ≤ 125 μm), As, Cr, and Ni exceeded the limit, even for the minimum values, while Cd, Pb and Hg were all lower than the reference values.

The ratios between the contaminant concentrations found in the bottom sediments and the legal limit defined for As, Cd, Cr, Hg, Ni, and Pb (Italian D.M. 367/03) shown in Fig. 6, have been calculated to better highlight the sediment contamination rate and its distribution in the study area. In the case of both the fine and coarse fractions (Fig. 6), Ni and Cr were always up to 11 and 6 times higher, respectively, than the legal limit, with the minimum values at Bianco station. The highest Ni values were concentrated in the bay, while the distribution of the highest Cr concentrations was wider and also included the northwestern coast. Pb was below the legal limit in the coarse fraction, while conversely As was slightly higher. In the fine fraction, As and Pb were higher than the legal limit at only a few stations, including Bianco station and the north-western areas (e.g. stations 15 and 16), but not in the bay. As already highlighted in Table 3, Hg and Cd were below the legal limit in both sediment fractions at all the stations. Hg, even if always under the legal limit, had its peak in the fine fraction of the Bianco station sediments.

There are no legal limits set for Cu and Zn, therefore the mean concentrations found in Bertolotto et al. (2005) off Riva Trigoso (eastwards of Sestri Levante, where there is a shipyard; Fig. 1) were considered as comparison values. These values correspond to the mean concentrations found in the sediments of three different stations sampled at 500, 700 and 1000 m from the shore. The resulting comparison values are 69.3 ppm of Cu and 111.3 ppm of Zn, and the ratios with the concentrations of this study were calculated and are shown in Fig. 7. Cu exceeded the comparison value more than Zn in the fine fraction, and, while Zn was higher than the comparison value at all the stations (with a decrease from W to E), Cu was lower than the comparison value at stations 13–16 and was more concentrated off the mouth of the Gromolo Torrent. In the coarse fraction, this metal exceeded the comparison value a few times, but only at Bianco station and inside the bay.
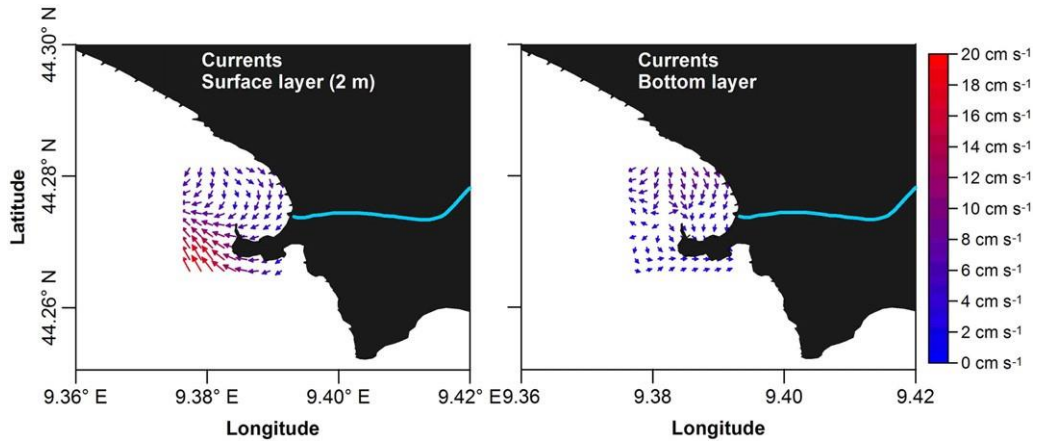
Fig. 4. Horizontal distribution of current vectors (in cm s^{-1}) in the surface layer (2 m-depth; left) and in the bottom layer (right).
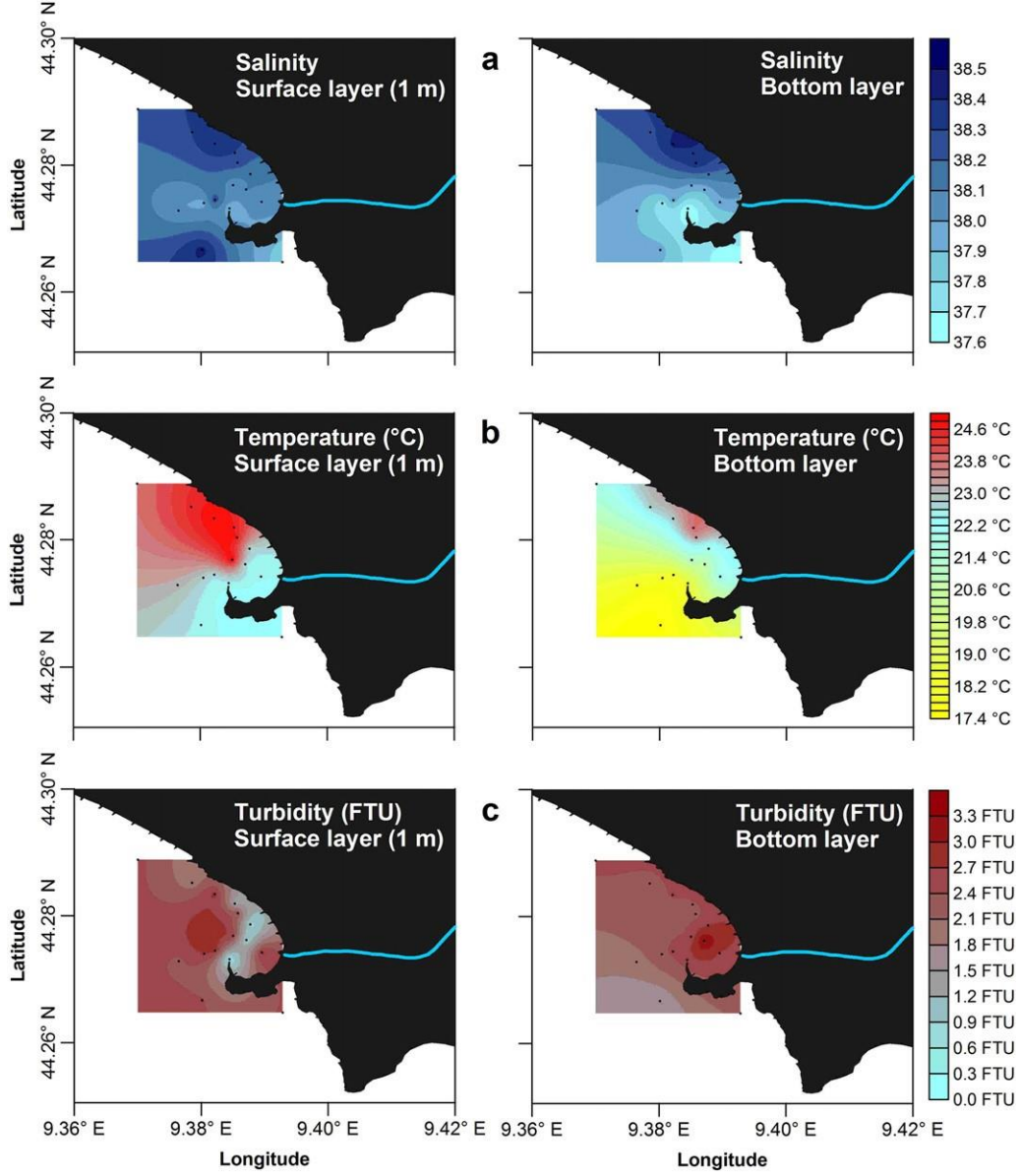

Fig. 5. Horizontal distribution of salinity (a), temperature, in °C (b) and turbidity, in FTU, (c) in the surface layer (0–1 m-depth; left) and in the bottom layer (right).

Table 3

Concentrations of the national regulatory guideline (Italian Ministerial Decree D.M. 367/03) and minimum, mean and maximum concentration of contaminants found in the two dimensional fractions studied (Ø b 63 μm and 63 ≤ Ø ≤ 125 μm) in the 16 samples of bottom sediments. Minimum and maximum values exceeding the legal limits are highlighted in bold. All values are reported in parts per million (ppm) of dry weight, except for Fe, reported in percentages (%), and Hg, reported in parts per billion (ppb).

|	As (ppm)	Cd (ppm)	Cr (ppm)	Cu (ppm)	Mn (ppm)	Ni (ppm)	Pb (ppm)	V (ppm)	Zn (ppm)	Hg (ppb)	Fe (%)
D.M. 367/03	12.0	0.30	50.0			30.0	30.0			300.0	
Ø b 63 μm fraction											
Minimum	9.3	0.07	103.2	56.2	538.0	99.0	16.6	38.0	111.4	20.0	3.3
Maximum	15.7	0.25	384.3	452.2	1207.0	342.5	43.3	241.0	262.7	285.0	8.8
Mean	12.4	0.11	295.8	158.4	927.9	269.6	23.8	71.9	167.3	90.7	4.5
Median	12.2	0.10	308.7	105.0	947.5	285.9	21.0	57.0	157.1	55.5	4.1
Standard deviation	2.0	0.05	63.5	128.7	153.4	65.5	6.9	47.3	43.8	72.9	1.2
63 ≤ Ø ≤ 125 μm fraction											
Minimum	12.1	0.03	75.5	26.8	299.0	64.8	13.9	26.0	78.7	7.0	1.8
Maximum	22.5	0.09	319.8	229.2	1099.0	339.8	23.9	98.0	195.5	24.0	4.9
Mean	17.1	0.06	271.0	78.8	849.8	271.4	17.0	55.1	111.7	14.2	3.6
Median	17.1	0.05	289.9	49.7	851.0	270.7	15.6	50.5	97.9	12.5	3.6
Standard deviation	2.9	0.02	59.3	63.2	178.9	62.6	3.4	18.7	36.5	4.6	0.7
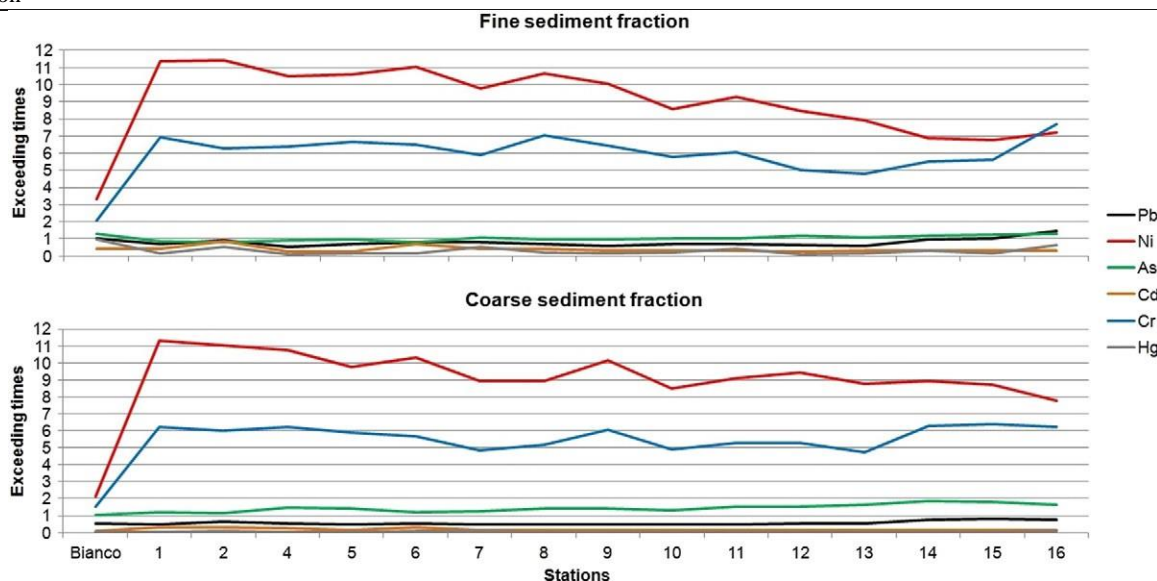
Fig. 6. Trend of the ratio between metal concentrations and legal limits (y axis) at all the study stations (x axis) in the fine (Ø b 63 μm, above) and coarse (63 ≤ Ø ≤ 125 μm, below) fractions.

The areal distribution of the metal concentrations in both the sediment fractions studied are shown in Fig. 8 (to simplify, only V, Cu, and Zn distributions are shown, while all the other metal maps are reported in the supplementary materials, Fig. S1 and Fig. S2). Generally, the fine fraction showed higher values than the coarse one, with the exception of As, which had higher concentrations in the coarse fraction. The distributions of the maximum concentrations were different for each of the metals. In the fine sediment fraction, As, Cr, Fe, Pb, and V had their maxima in the western stations, while Cd, Cu, Mn, and Ni had theirs inside the bay. In the coarse fraction, As, Cr, Fe, Hg, Mn, Pb and V had their maximum in the western part of the study area, while Cu, Ni, and Cd had their highest values off the mouth of

the Gromolo Torrent. Bianco station had the highest concentration of Zn (263 ppm) and Hg (285 ppb) in the fine fraction, and Zn (196 ppm) in the coarse fraction, but the lowest values of Cr, Fe, Mn, Ni, and V in the fine fraction, and As, Cr, Cd, Fe, Mn, Ni, and V in the coarse fraction.

The mineralogy of the marine sediments was characterised by a general homogeneity, both at the different stations and in the different analysed fractions (Table 4a and Table 4b). Quartz and illite were the main phases inside the sediments in both fractions, followed by albite and chlorite. Calcite, serpentine and talc were also present in all the samples, with the exception of talc in the fine fraction at Bianco station. Amphibole was another common mineral, while pyroxenes and, to a

minor extent, calcite tended to concentrate in the fine fraction. Neither amphibole nor pyroxenes were detected at the Bianco sampling point, and serpentine seemed to be present in smaller amounts than at the other stations, especially in the coarse fraction while, on the contrary, talc and albite reached their maximum concentration in this fraction. It is worth noting that cuprite, a mineral deriving from AMD-related precipitates, was detected only at station 1, while hematite, magnetite, and garnet were detected only at stations 15 and 16.

Pearson's correlation coefficient matrix was used to evaluate the relationships between the observed metals, the mineralogical composition of the sediments, and the physical-chemical properties (T and Sal) of the water in the bottom layer of the water column (Tables 5a and 5b). In particular, the correlation analysis was conducted to determine the eventual influence of physical-chemical parameters of the bottom water (Nicolau et al., 2006) and the mineralogical characteristics of the sediments (Cox and Preda, 2003) on the metal concentrations.

In the fine fraction (Table 5a), two different but related groups of elements were observed: the first group contained Fe, V, Pb, As, and Mn, while the second group contained Cu, Zn, Cd, and Ni. Hg, Cr, and, to some extent, Ni tended to be correlated with elements belonging to both groups. Arsenic showed a high negative correlation with Cu and Ni ($r = -0.72$ and -0.88, respectively). The only mineral showing a positive correlation with some elements, in particular As, Hg, and less clearly Pb, was chlorite.

Some positive and negative correlations found in the fine fraction were also observed in the coarse one (Table 5b), but new relationships were highlighted, primarily between Zn-Cu, and between Mn, Fe, As, V, and Cr. As in the case of the fine fraction, two groups of metals could be distinguished in the coarse fraction: Fe, V, Pb, As, and Mn were again positively correlated with each other, but Cr and Ni also belonged to this group; while the second group was composed of Cu, Zn, Cd, and Hg. In the fine fraction, Ni and Cu showed an $r = 0.60$

due to their concentration in the stations with the maximum percentage of fine sediments, while they were not correlated in the coarse fraction. In the coarse fraction, chlorite was again the only mineral presenting a positive correlation with metals, although in this fraction it was correlated to Ni and Cd.

With regard to the influence of the physical-chemical parameters of the water, in the fine fraction, T and Sal showed a negative correlation with Zn and Hg (Table 5a). In the coarse fraction, Mn, Fe, As, and Cr were positively linked to both T and Sal, while Zn was again negatively correlated to the physical characteristics of the water (Table 5b).

The principal component analysis (PCA) was used to highlight the main differences between the sample stations and summarise their characteristics and their possible grouping. The PCA results are shown in Fig. 9 and Fig. 10 for the fine and coarse sediment fractions, respectively. In the fine fraction, the first three principal components explain a cumulative variance in the data of 80.04% (factor1: 32.76%, factor 2: 26.30%, and factor 3: 20.98%) and clearly separate Bianco station, characterised by Zn, Hg, illite and chlorite, from the group of western stations (14–16), characterised by Fe, V, As, and Pb, and from stations 2 and 6, and, to a minor extent, station 1, off the mouth of the torrent, due to the presence of Cu, Cd, Ni and quartz.

In the coarse sediment fraction (Fig. 10), the first three principal components explain a cumulative variance in the data of 78.89% (factor 1: 41.08%, factor 2: 24.18%, and factor 3: 13.63%) and show a similar separation in the fine fraction (Fig. 9), confirming the different characteristics of the different groups of stations and the different inputs of contaminants to which they are subjected. In fact, also in this case, Bianco station was clearly separated from all the other stations, as well as the group of western stations (from 14 to 16), and stations 1, 2 and 6 off the mouth of the Gromolo Torrent.

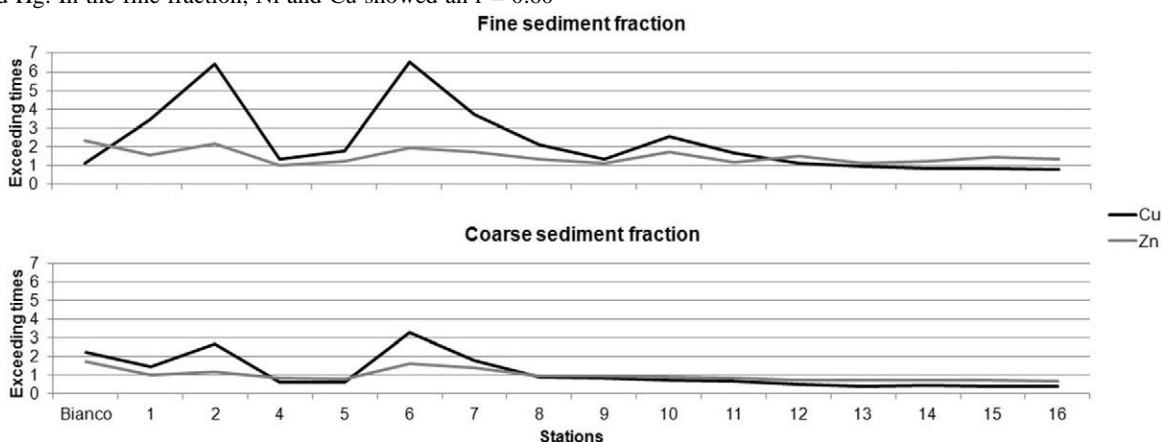Fig. 7. Trend of the ratio between metal concentrations and mean values found in Bertolotto et al. (2005) (y axis) at all the study stations (x axis) in the fine (Ø b 63 μm, above) and coarse (63 ≤ Ø ≤ 125 μm, below) fractions.
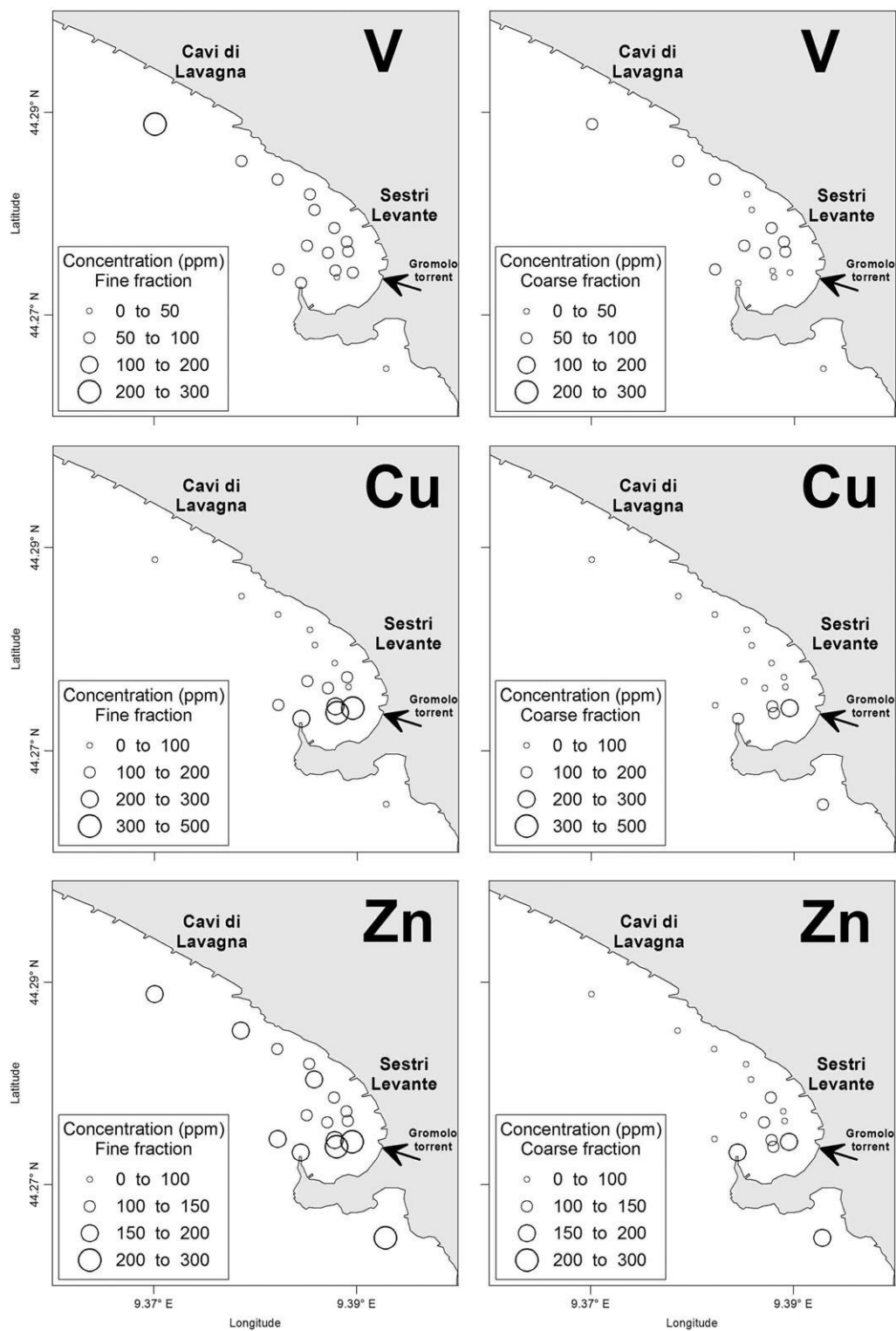
Fig. 8. Distribution of V, Cu, and Zn concentrations in the study area in the fine fraction (Ø b 63 μm; on the left) and in the coarse fraction (63 ≤ Ø ≤ 125 μm; on the right). Concentrations are
in ppm.

Table 4a
Summary table of the mineralogical features of the fine (Ø b 63 μm) fraction of the bottom sediment samples. Values are expressed in percentage; values equal to zero have not been reported.

	Sampling stations															
Minerals	Bianco	1	2	4	5	6	7	8	9	10	11	12	13	14	15	16
Quartz	27	28	34	36	39	34	31	34	36	34	38	33	33	29	33	30
Calcite	5	3	3	3	3	2	3	4	4	3	3	2	3	3	3	2
Albite	13	11	5	15	11	11	15	9	13	14	9	15	10	16	9	9
Talc		4	2	4	2	2	2	2	2	2	2	3	2	2	2	6
Chlorite	16	7	11	6	9	9	10	10	6	10	10	10	12	13	13	10
Illite	37	27	28	33	32	32	31	30	28	36	33	32	28	26	29	26
Serpentine	2	3	4	3	3	3	3	3	3	2	3	3	2	2	2	1
Amphibole		2	2		2	3		3	2			3	2	2	3	4	3
Diopside		5				5	6		6					8	6	6	6
Ortopyroxene		11	11					6								
Magnetite																2
Garnet																4
Hematite																1

Discussion

The distribution of the dimensional classes of the bottom sediments (Fig. 3), with high percentages of fine sediments inside the bay, is in agreement with the bathymetry of the bottom found by Di Matteo and Milli (2008). This is also in agreement with the coastal topography and the slow currents of the area (Fig. 4) that control the distribution of the chemical-physical parameters of the sea water (Fig. 5a-b) and the dispersion of the sediment and torrent discharge, allowing the transport and deposition of fine material inside the bay. This phenomenon is also confirmed by the distribution of the turbidity (Fig. 5c) that has higher values inside the bay than outside it.

The high level of Ni and Cr found in the sediments in the entire study area (Fig. 6) agrees with the bulk chemistry composition of the rocks outcropping in the area; in fact, ophiolite-related soils and stream sediments contain very high concentrations of these two metals (Albanese et al., 2015). Moreover, these elements tend to be concentrated in the sediments as they are not easily soluble and their related minerals (for example, chromite and serpentine) are stable under these conditions (Albanese et al., 2015). The high values of As and Pb, found at the southeastern and northwestern extremities of the study area, suggest that these elements are not derived from the mine discharge or the mineralogy of the area. Moreover, Zaccarini and Garuti (2008) and Carbone et al. (2012) demonstrated that only very small quantities of As and Pb were present in the sulphide mineralisations of the Libiola mining area. Arsenic sources could be related to industry as observed by Amano et al. (2011) and Pb is both produced by and used in different industrial activities (such as the burning of coal and oil fuel, painting, electronics, alloys, etc.) and is also involved in different biological processes (e.g. associated with marine plankton) (Amano et al., 2011). In our case, they were probably due to human activities along this section of the coast (ports, cities, etc.) or inputs from sources further to the west (e.g. the Entella Torrent). The high Hg content at Bianco station may be partly explained by the presence of the nearby sewage outlet (Fig. 1); in fact, as indicated by Shoham-Frider et al. (2007), half of the Hg in the sewage can derive from municipal households, drinking water supply systems, dental clinics and industrial sources (such as caustic soda production), while the source of the other half is unknown.

	Sampling stations															
Minerals	Bianco	1	2	4	5	6	7	8	9	10	11	12	13	14	15	16
Quartz	33	38	35	35	32	36	37	39	30	35	37	33	37	30	30	30
Calcite	1	2	1	2	1	2	2	2	2	2	2	2	3	2	2	3
Albite	18	6	9	16	5	9	12	10	13	12	7	14	10	8	13	12
Talc	10	7	3	4	1	2	5	3	7	5	4	5	2	2	3	5
Chlorite	4	8	8	6	5	8	6	6	6	8	5	6	7	6	6	6
Illite	33	35	36	34	28	38	30	38	31	33	31	35	35	40	38	30
Serpentine	1	4	4	3	2	3	2	2	2	2	2	2	2	2	2	2
Amphibole		5	1	1	3	6	1	2	3	2	3	4	2	1	2	
Diopside					25				8		11			8	5	10

Magnetite   1

Hematite   1

Cuprite   1

Table 5a

Pearson's correlation coefficients among metal concentrations in the sediments, physical-chemical parameters of the bottom water and mineralogical characteristics of the sediments. Observation number: 17. Significant and strong correlations (positive or negative) are marked in bold at the 0.05 level and in italic bold at 0.01 level. Sediment fraction: Ø b 63 μm. T: water temperature; S: water salinity.

	Cu	Pb	Zn	Ni	Mn	Fe	As	Cd	V	Cr	Hg	Quartz	Albite	Chlorite	Illite	T	Sal
Cu	1.00																
Pb	−0.06	1.00															
Zn	0.59	0.34	1.00														
Ni	0.60	−0.50	−0.22	1.00													
Mn	−0.11	0.20	−0.41	0.26	1.00												
Fe	−0.21	0.77	−0.15	−0.20	0.58	1.00											
As	−0.72	0.61	−0.02	−0.88	0.17	0.48	1.00										
Cd	0.90	0.19	0.68	0.34	−0.28	−0.11	−0.52	1.00									
V	−0.30	0.78	−0.20	−0.25	0.51	0.99	0.52	−0.16	1.00								
Cr	0.26	0.02	−0.44	0.75	0.60	0.46	−0.44	0.10	0.42	1.00							
Hg	0.03	0.64	0.60	−0.56	−0.20	0.23	0.44	0.27	0.24	−0.45	1.00						
Quartz	0.03	−0.52	−0.46	0.51	0.06	−0.20	−0.47	−0.11	−0.21	0.36	−0.48	1.00					
Albite	−0.35	−0.26	−0.16	−0.24	0.04	−0.18	0.24	−0.52	−0.18	−0.30	−0.14	−0.20	1.00				
Chlorite	−0.19	0.49	0.47	−0.79	−0.24	0.03	0.64	0.09	0.05	−0.72	0.60	−0.47	−0.10	1.00			
Illite	−0.01	−0.27	0.38	−0.25	−0.50	−0.42	0.01	−0.11	−0.42	−0.55	0.22	0.18	0.32	0.18	1.00		
T	−0.23	−0.10	−0.67	0.20	0.22	0.13	−0.03	−0.23	0.17	0.30	−0.65	0.31	−0.24	−0.19	−0.69	1.00	
Sal	−0.45	−0.04	−0.69	0.01	0.23	0.24	0.17	−0.46	0.27	0.23	−0.63	0.19	−0.04	−0.11	−0.64	0.90	1.00

The comparison of Cu and Zn concentrations with the values found in Bertolotto et al. (2005) (Fig. 7) highlights how Zn and Cu have the highest values inside the Sestri Levante bay and are more linked to the residual fraction than the coarse fraction of the sediments, as already found in Yuan et al. (2004).

This situation confirms that their distribution is strongly influenced by the currents of the area and the resulting distribution of sediments: in fact, they have accumulated inside the bay where the current intensity is minimal and the fine sediments are concentrated, and have lower concentrations along the north-western coast where the currents are stronger and the effect of waves on sediment resuspension and metal remobilisation is greater (Duran et al., 2012).

The fact that both metals show their highest values in the two stations nearest the mouth of the Gromolo Torrent (stations 2 and 6) is evidence that they derived from the torrent input. Naturally, Cu can be discharged into the environment from forest fires, weathering process of exposed soil, and decaying vegetation, while anthropogenic sources of Cu may come from domestic use of Cu-based chemicals, untreated municipal sewage sludge, and corrosion of Cu materials (Shaari et al., 2015). Instead, the possible sources of Zn are motor oil and grease, fertilizers, sewage sludge, transmission fluid and concrete (Shaari et al., 2015). Moreover, landfill leachate and iron hydroxides can transport and adsorb, respectively, large quantities of metals, and iron oxides can also play an important role in trapping metals in aquatic sediments (Guigue et al., 2013; Salomons and Forstner, 1984). However, in the case of Sestri Levante, all the above-mentioned processes can explain only a small part of the Cu and Zn in comparison

to the huge quantity of these metals derived from the pyrite and chalcopyrite mineralisations of the Libiola mine discharge and transported by the Gromolo Torrent to the sea (Dinelli et al., 2001; Zaccarini and Garuti, 2008).

The interpretation of Pearson's coefficients (Tables 5a and 5b) was elaborated because of the complexity of the sedimentology of the area and the multitude of processes taking place, such as biological activity and absorption, which have an especially important role in the fine fraction. Nevertheless, the first difference resulting from the comparison of the correlations in the two considered sediment

fractions is the large number of good correlations in the coarse fraction. These correlations are found among the metals themselves, but also between the metals and the chemical-physical parameters of the water. These metal correlations with the chemical-physical parameters of the water could be due to the fact that some elements, such as Cu and Zn, for example, display similar behaviour in similar condition (Duran et al., 2012).

Table 5b Pearson's correlation coefficients among metal concentrations in the sediments, physical-chemical parameters of the bottom water and mineralogical characteristics of the sediments. Observation number: 17. Significant and strong correlations (positive or negative) are marked in bold at the 0.05 level and in italic bold at 0.01 level. Sediment fraction: $63 \le \varnothing \le 125$ μm. T: water temperature; S: water salinity.

|	Cu	Pb	Zn	Ni	Mn	Fe	As	Cd	V	Cr	Hg	Quartz	Albite	Chlorite	Illite	T	Sal
Cu	1.00																
Pb	−0.19	1.00															
Zn	0.90	−0.30	1.00														
Ni	−0.04	−0.08	−0.38	1.00													
Mn	−0.57	0.51	−0.75	0.57	1.00												
Fe	−0.46	0.73	−0.64	0.42	0.93	1.00											
As	−0.79	0.57	−0.81	0.16	0.84	0.78	1.00										
Cd	0.57	−0.05	0.22	0.68	0.03	0.04	−0.37	1.00									
V	−0.51	0.83	−0.59	0.12	0.81	0.94	0.78	−0.16	1.00								
Cr	−0.29	0.35	−0.60	0.86	0.84	0.80	0.50	0.46	0.60	1.00							
Hg	0.51	0.27	0.35	0.14	0.05	0.23	−0.31	0.43	0.21	0.22	1.00						
Quartz	0.32	−0.67	0.29	0.18	−0.28	−0.50	−0.44	0.31	−0.65	−0.24	−0.07	1.00					
Albite	−0.01	0.07	0.23	−0.55	−0.37	−0.27	−0.09	−0.37	−0.09	−0.48	−0.02	−0.25	1.00				
Chlorite	0.34	−0.05	0.00	0.61	0.18	0.20	−0.18	0.71	−0.02	0.43	0.26	0.32	−0.32	1.00			
Illite	0.15	0.35	0.02	0.10	0.18	0.20	0.24	0.27	0.14	0.11	−0.24	0.08	−0.01	0.37	1.00		
T	−0.42	0.42	−0.62	0.58	0.66	0.57	0.74	0.37	0.47	0.65	−0.20	−0.29	−0.42	0.23	0.41	1.00	
Sal	−0.65	0.50	−0.80	0.47	0.67	0.63	0.83	0.12	0.57	0.63	−0.32	−0.46	−0.30	0.26	0.40	0.90	1.00
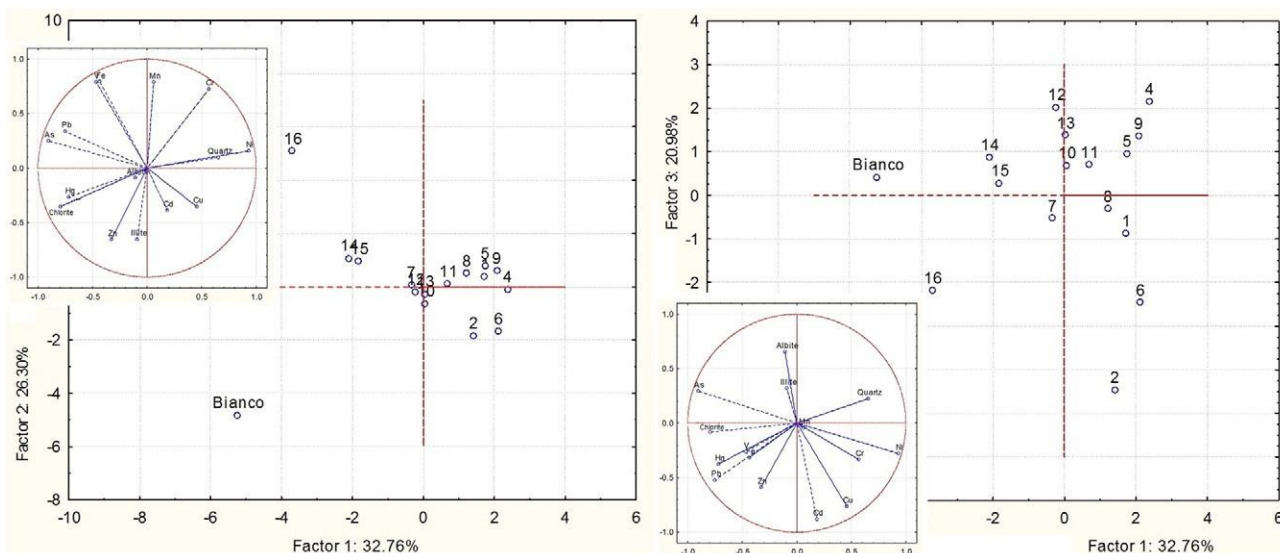
Fig. 9. Results of Principal Component Analysis (PCA) of 15 metal and mineralogical parameters from the fine fraction (Ø b 63 μm) of the sediments.

Moreover, the presence of two similar groups of correlated metals in both the fractions suggests that two different metal sources can be distinguished. In the fine fraction (Table 5a), the high negative correlation found between As and Cu and Ni suggests that these metals could have originated from different sources (Shaari et al., 2015). The positive correlation between chlorite and As, Hg and Pb could be explained by adsorption processes (Lin and Puls, 2000; Wainipee et al., 2013). It is worth noting that neither the clay minerals (illite) nor the other minerals show any positive correlation with the metal content. This fact may be explained by the low capacity of these minerals to host in their crystalline structures or selectively absorb metals (Alamgir, 2016).

The close association of Ni and Cr in both the fractions could be due to their very similar areal distribution in the sediments, and this is further evidence of their coming from the same source and their common dispersion by the dynamics of the area (Albanese et al., 2015). Because Mn does not derive from the mine discharge (Carbone et al., 2013), the appearance of this element in the positive relationship in the coarse fraction (Table 5b) can be explained by the chemical composition and

diagenesis of the sediment that could affect the metal accumulation process (Shaari et al., 2015). The positive correlation between Chlorite, Ni and Cd in this fraction may be due to incorporation processes, as this mineral can host Ni and almost every transition metal in its structure (Bailey, 1988).

According to the correlation between metals and physicalchemical water parameters, the metals present in the coarse fraction seem to be more affected by the temperature and salinity of the bottom water than the elements found in the fine fraction. This situation could be caused by the similar distribution of the coarse fraction, metals such as Mn, Fe, and As, and the physicalchemical parameters of the water in the study area; in fact, thanks to the currents and the more intense hydrodynamism present in the northern sector of the study area, the coarse fraction is more concentrated there, and in the presence of this abundant coarse fraction both the temperature and salinity and the aforementioned metals have high values.

The differences observed in the PCA (Figs 9 and 10) at Bianco station could be related to the presence of the sewage outlet, as previously mentioned, and the different mineralogy due to the extensive presence in the this area of shales (Bortolotti et al., 2014), rich in
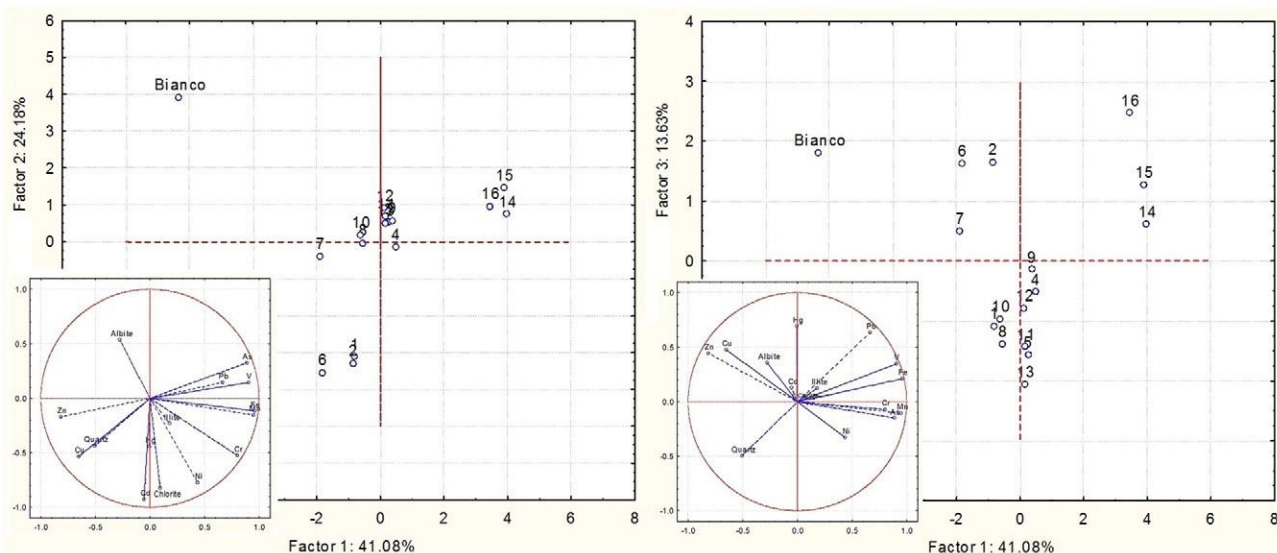

Fig. 10. Results of Principal Component Analysis (PCA) of 15 metal and mineralogical parameters from the coarse fraction (63 ≤ Ø ≤ 125 μm) of the sediments.

phyllosilicates (mica and chlorite), whose alteration pathway is mainly illite.

The different metal values recorded at stations 14–16, particularly for Fe, Pb, and V, may be related to the sediments carried by the eastward counter-current which carries coastal material from the mouth of the Entella Torrent, testified to by the presence of hematite and magnetite in both the sediment fractions (Tables 4a and 4b). In fact, these minerals are present in the formations of the Entella Torrent catchment area that is divided into three sub-basins characterised by: 1)Cretaceous silty flysch sedimentary formations and significant alluvial, colluvial, and eluvial debris deposits, and a succession of argillite shales;2) formations of Palombini Shale and Sandstones from Mount Gottero; 3) outcrops of ophiolitic sequences that consist of peridotites, gabbros, and jasper, and Calpionella Limestone (Barsanti et al., 2003; Ducci et al., 1995).

Stations 1, 2, and 6, the nearest to the mouth of the Gromolo Torrent, are more affected by the materials carried by this torrent, which are characterised by very high concentrations of Cd, Cu, and Zn, coming from the Libiola mine mineralisations (Dinelli et al., 2001). These elements could be related to the presence of chlorite, as already suggested by the correlation matrix, but the concentration of these minerals is fairly constant in the study area. The presence of small amounts of amorphous, metal-rich colloids, transported by the Gromolo Torrent (Dinelli and Tateo, 2002) and deposited at its mouth is supported by the situation found at these stations.

Finally, to evaluate the degree of contamination of the Sestri Levante sediments, a comparison of metal compositions found in this study with other research carried out in regions with different values of crustal metals, as well as different human activities, was made. An overview of the mean concentrations of metals found in the bottom sediments of different natural and anthropic sites in Italy and in the rest of the world, is reported in Table 6. Some concentrations measured in this study are lower than or comparable to those found in the less disturbed sediments: e.g. Cd, despite having relatively higher concentrations near the mouth of the Gromolo Torrent than outside the bay (Fig. S1), has values under the legal limit and also similar to concentrations measured at the Archipelago of La Maddalena (Schintu et al., 2015). Conversely, other metals show higher concentrations than those measured in strongly impacted sites in the world, such as Cr, Cu, Ni, and Mn in the Gulf of Izmir (Turkey; Bergin et al., 2006) or Beppu Bay (Japan; Amano et al., 2011). These different conditions show that any contamination is site-specific, depending on the human activities that are the vehicle of contamination input and the mineralogical characteristics of the area that is the natural source of the metals (Van Meirvenne and Goovaerts, 2001).

The complexity of the study of metal sources is highlighted by the very different results found in various parts of the world, but notably different results can also found within a small area, as in the case of Sestri Levante. In fact, here, within a few kilometres, different mineralogical compositions, inputs from very different human activities, inputs from different torrents and complex marine dynamics, due to the presence of bays and headlands, produce a complex situation that makes the determination of metal sources very difficult. 6. Conclusions

This preliminary study of the distribution of contaminants in the bottom sediments of the "Baia delle Favole" of Sestri Levante (Italy) shows the existence of a high concentrations of Cu and Zn, and relatively high concentrations of Cd and Ni in the bay, especially off the mouth of the Gromolo Torrent, whose catchment area includes the mineralisations of the Libiola mine. During this study, high concentrations of As, Cr, Hg, Mn, Pb, and V were also found in the northern part of the study area and, in some cases, to the east (Bianco station). These contaminants are not attributable to the Gromolo Torrent input, but some could be attributable to the discharge of the nearby Entella Torrent and/or other source (such as sewage).

The subdivision of the study stations obtained from the Principal Component Analysis highlights the complex set of factors that affects the distribution of metals and minerals in the area and the influence of the currents on the dispersion of these in the area.

Due to the interesting characteristics found in the stations at the edge of the study area, a more extensive study, both westwards and eastwards is essential to better understand the source of the contaminants found in the bottom sediments.

Moreover, based on the results obtained from this study, additional research is needed to highlight the possible seasonal differences in the contributionofthe GromoloTorrent tothe metalcontent of thebottomsediments in the coastal area. In fact, as the Libiola mine and the Gromolo Torrent belong to the Mediterranean area, characterised by notable variations in rainfall patterns with long dry spells (when the torrent waters are at their lowest) interrupted by short periods of heavy rain (often causing severe floods), some seasonal differences could be found in the metal input from the mine to the torrent and, successively, from the torrent to the sea.

Table 6 Mean concentrationsof metals found in bottom sediments sampled in natural and contaminated area in the world. Values area expressed in ppm of dry weight, with the exception of Fe (in %) and Hg (in ppb); n.a.: values not available.

References	Study area	Characteristics of the study area	As (ppm)	Cd (ppm)	Cr (ppm)	Cu (ppm)	Fe (%)	Hg (ppb)	Pb (ppm)	Zn (ppm)	Ni (ppm)	Mn (ppm)	V (ppm)
This study	Sestri Levante, Italy	Ø b 63 µm fraction	12.4 ± 2.0	0.1 ± 0.0	295.8 ± 63.5	158.4 ± 128.7	4.5 ± 1.2	90.7 ± 72.9	23.8 ± 6.9	167.3 ± 43.8	269.6 ± 65.5	927.9 ± 153.4	71.9 ± 47.3
This study	Sestri Levante, Italy	63 ≤ Ø ≤ 125 µm fraction	17.1 ± 2.9	0.1 ± 0.0	271.0 ± 59.3	78.8 ± 63.2	3.6 ± 0.7	14.2 ± 4.6	17.0 ± 3.4	111.7 ± 36.5	271.4 ± 62.6	849.8 ± 178.9	55.1 ± 18.7
Bertolotto et al., 2005	Chiavari, Italy	Between 500 and 1000 m from the coast	9.7 ± 2.1	0.4 ± 0.3	196.7 ± 49.3	31.0 ± 2.6	n.a.	57.7 ± 25.2	34.3 ± 5.9	126.7 ± 15.3	n.a.	n.a.	n.a.
Bertolotto et al., 2005	Riva Trigoso, Italy	Between 500 and 1000 m from the coast	10.3 ± 2.1	0.6 ± 0.4	423.3 ± 121.0	69.3 ± 4.2	n.a.	90.0 ± 17.3	41.0 ± 4.0	111.3 ± 33.8	n.a.	n.a.	n.a.
Romano et al., 2008	Bagnoli, Naples, Italy	Industrial area	54.7 ± 17.7	0.4 ± 0.3	24.5 ± 8.0	41.5 ± 70.3	n.a.	350.7 ± 286.8	187.4 ± 118.3	591.8 ± 591.9	n.a.	n.a.	n.a.
Guerra et al., 2009	Pialassa Baiona, Ravenna, Italy	Eutrophic lagoon system	n.a.	2.2 ± 0.1	90.3 ± 4.2	244.0 ± 9.0	n.a.	2900 ± 200	117.0 ± 2.0	n.a.	31.6 ± 2.4	n.a.	n.a.
Schintu et al., 2015	Portoscuso, Sardinia, Italy	Industrial district of Portovesme	8.4 ± 8.4	2.2 ± 3.2	11.6 ± 18.5	12.9 ± 27.2	0.4 ± 0.5	800 ± 1300	45.8 ± 46.1	172.6 ± 280.0	n.a.	n.a.	n.a.
Schintu et al., 2015	Porto Torres, Sardinia, Italy	Industrial and civilian port	5.2 ± 2.0	0.2 ± 0.1	27.4 ± 25.3	16.7 ± 13.2	1.0 ± 0.7	1300 ± 2100	16.1 ± 12.1	72.9 ± 32.6	n.a.	n.a.	n.a.
Schintu et al., 2015	La Maddalena Archipelago, Sardinia, Italy	SCI - Site of Community Importance	8.4 ± 6.5	0.1 ± 0.0	21.5 ± 19.1	44.7 ± 65.2	0.7 ± 0.5	600 ± 1000	31.8 ± 26.1	63.1 ± 70.8	n.a.	n.a.	n.a.
Bergin et al., 2006	Gulf of Izmir, Western Turkey	Densely populated and industrialised area	n.a.	0.0 ± 0.0	109.6 ± 42.7	22.4 ± 12.4	n.a.	200 ± 100	48.4 ± 14.9	99.9 ± 55.8	108.1 ± 42.3	511.1 ± 149.4	n.a.
Martins et al., 2012	Portugal	Oceanic coast	13.2 ± 12.7	n.a.	48.0 ± 27.5	8.8 ± 6.3	n.a.	n.a.	25.9 ± 17.6	42.8 ± 38.0	8.1 ± 5.8	n.a.	35.7 ± 27.0
Cox and Preda, 2003	Gulf of Carpentaria, Australia	The largest embayment on the coastline of the Australian continent.	n.a.	n.a.	42 ± 1.2	289 ± 6	n.a.	n.a.	166 ± 7	346 ± 8	25 ± 0.7	n.a.	n.a.
Zhu et al., 2012	Xiawan Port, China	Industry zone	n.a.	70.0 ± 66.0	n.a.	302.0 ± 109.9	n.a.	n.a.	502.0 ± 335.5	2840.0 ± 1650.2	n.a.	n.a.	n.a.
Buruaem et al., 2012	Mucuripe harbour, Brazil	Commercial harbour	n.a.	0.9 ± 0.3	25.4 ± 16.4	8.5 ± 6.1	n.a.	40 ± 10	3.3 ± 1.7	310.4 ± 200.3	14.1 ± 6.0	n.a.	n.a.
Buruaem et al., 2012	Pecém harbour, Brazil	Industrial complex	n.a.	0.9 ± 0.5	42.3 ± 19.7	13.1 ± 5.7	n.a.	40 ± 10	n.a.	463.9 ± 187.8	18.8 ± 6.6	n.a.	n.a.
Buruaem et al., 2012	Santos harbour, Brazil	Commercial and industrial harbour	n.a.	n.a.	32.3 ± 6.6	16.2 ± 7.0	n.a.	260 ± 230	12.3 ± 4.0	787.2 ± 227.3	14.2 ± 4.9	n.a.	n.a.
Shaari et al., 2015	East Coast of Peninsular Malaysia	Exclusive economic zone	n.a.	n.a.	n.a.	17.48 ± 2.14	7.6 ± 0.5	n.a.	n.a.	63.01 ± 15.49	n.a.	273.4 ± 57.9	n.a.
Amano et al., 2011	Beppu Bay, Japan	Industrial zone	11.6 ± 4.3	0.3 ± 0.1	43.8 ± 10.0	33.4 ± 3.1	n.a.	n.a.	28.5 ± 2.0	129.2 ± 9.2	n.a.	801.3 ± 507.8	70.8 ± 9.9

References

Accornero, M., Marini, L., Ottonello, G., Vetuschi Zuccolini, M., 2005. The fate of major constituents and chromium and other trace elements when acid waters from the derelict Libiola mine (Italy) are mixed with stream waters. Appl. Geochem. 20, 1368–1390. http://dx.doi.org/10.1016/j.apgeochem.2005.03.001.

Adlassnig, W., Sassmann, S., Grawunder, A., Puschenreiter, M., Horvath, A., KollerPeroutka, M., 2013. Amphibians in Metal-contaminated Habitats. Salamandra. 49(3) pp. 149–158 (ISSN: 0036-3375).

Akcil, A., Koldas, S., 2006. Acid mine drainage (AMD): causes, treatment and case studies. J. Clean. Prod. 14, 1139–1145. http://dx.doi.org/10.1016/j.jclepro.2004.09.006.

Alamgir, M., 2016. The Effect of Soil Properties to the Extent of Soil Contamination with Metals. Springer Ed., Environmental Remediation Technologies for MetalContaminated Soils. Tokyo, Japan, pp. 1–20 http://dx.doi.org/10.1007/978-4-43155759-3.

Albanese, S., Sadeghi, M., Lima, A., Cicchella, D., Dinelli, E., Valera, P., Falconi, M., Demetriades, A., De Vivo, B., The GEMAS Project Team, 2015. GEMAS: cobalt, Cr, Cu and Ni distribution in agricultural and grazing land soil of Europe. J. Geochem. Explor. 154, 81–93. http://dx.doi.org/10.1016/j.gexplo.2015.01.004.

Amano, A., Kuwae, M., Agusa, T., Omori, K., Takeoka, H., Tanabe, S., Sugimoto, T., 2011. Spatial distribution and corresponding determining factors of metal concentrations in surface sediments of Beppu Bay, Southwest Japan. Mar. Environ. Res. 71, 247–256. http://dx.doi.org/10.1016/j.marenvres.2011.01.009.

Asta, M.P., Calleja, M.L., Pérez-Lopez, R., Auqué, L.F., 2014. Major hydrogeochemical processes in an acid mine drainage affected estuary. Mar. Pollut. Bull. 91 (1), 295–305. http://dx.doi.org/10.1016/j.marpolbul.2014.11.023.

Bailey, S.W., 1988. Chlorites: Structures and Crystal Chemistry. In: Bailey, S.W. (Ed.), Hydrous Phyllosilicates (Exclusive of Micas) Vol. 19. Reviews in Mineralogy and Geochemistry, Mineralogical Society of America, Chantilly, Virginia, pp. 347–403.

Baker, B.J., Tyson, G.W., Goosherst, L., Banfield, J.F., 2009. Insights into the diversity of eukaryotes in acid mine drainage biofilm communities. Appl. Environ. Microbiol. 75 (7), 2192–2199. http://dx.doi.org/10.1128/AEM.02500-08.

Barsanti, M., Delbono, I., Ferretti, O., Zaquini, M., Setti, M., 2003. Caratterizzazione Della Piattaforma Costiera Antistante la Foce dell'Entella Tramite Parametri Mineralogici e Granulometrici. Volume ENEA, Studi per la creazione di strumenti della gestione costiera - Golfo del Tigullio, Eds ENEA, In, pp. 84–99.

Bergin, F., Kucuksezgin, F., Uluturhan, E., Barut, I.F., Meric, E., Avsar, N., Nazik, A., 2006. The response of benthic foraminifera and ostracoda to heavy metal pollution in gulf of Izmir (eastern Aegean Sea). Estuar. Coast. Shelf Sci. 66, 368–386. http://dx.doi.org/ 10.1016/j.ecss.2005.09.013.

Bertolotto, R.M., Tortarolo, B., Frignani, M., Bellucci, L.G., Albanese, S., Cuneo, C., AlvaradoAguilar, D., Picca, M.R., Gollo, E., 2005. Heavy metals in surficial coastal sediments of the Ligurian Sea. Baseline. Mar. Pollut. Bull. 50, 344–359.

Blowes, D.W., Ptacek, C.J., Jambor, J.L., Weisener, C.G., 2003. The Geochemistry of Acid Mine Drainage. Treatise on Geochemistry Volume 9: Environmental Geochemistry. pp. 149–204 http://dx.doi.org/10.1016/B0-08-043751-6/09137-4.

Bortolotti, V., Mannori, G., Piccini, L., Aiello, I.W., Chiari, M., Principi, G., Reale, V., 2014. Note Illustrative Alla Carta Geologica d'Italia Alla Scala 1:50000, Foglio 232, Sestri Levante (http://www.isprambiente.gov.it/Media/carg/note_illustrative/232_ Sestri_ Levante.pdf).

Buruaem, L.M., Hortellani, M.A., Sarkis, J.E., Costa-Lotufo, L.V., Abessa, D.M.S., 2012. Contamination of port zone sediments by metals from large marine ecosystems of Brazil. Mar. Pollut. Bull. 64, 479–488. http://dx.doi.org/10.1016/j.marpolbul.2012.01. 017.

Cantonati, M., Angeli, N., Virtanen, L., Wojtal, A.Z., Gabrieli, J., Falasco, E., Lavoie, I., Morin, S., Marchettoh, A., Fortin, C., Smirnova, S., 2014. Achnanthidium minutissimum (Bacillariophyta) valve deformities as indicators of metal enrichment in diverse widely-distributed freshwater habitats. Sci. Total Environ. 475, 201–215. http://dx. doi.org/10.1016/j.scitotenv.2013.10.018.

Carbone, C., Di Benedetto, F., Marescotti, P., Martinelli, A., Sangregorio, C., Cipriani, C., Lucchetti, G., Romanelli, M., 2005. Genetic evolution of nanocrystalline Fe oxide and oxyhydroxide assemblages from the Libiola mine (eastern Liguria, Italy): structural and microstructural investigations. Eur. J. Mineral. 17, 785–795.

Carbone, C., Marescotti, P., Lucchetti, G., Martinelli, A., Basso, R., Cauzid, J., 2012. Migration of selected elements of environmental concern from unaltered pyrite-rich mineralizations to Fe-rich alteration crusts. J. Geochem. Explor. 114, 109–117. http://dx.doi. org/10.1016/j.gexplo.2012.01.003.

Carbone, C., Dinelli, E., Marescotti, P., Gasparotto, G., Lucchetti, G., 2013. The role of AMD secondary minerals in controlling environmental pollution: indications from bulk leaching tests. J. Geochem. Explor. 132, 188–200. http://dx.doi.org/10.1016/j.gexplo. 2013.07.001.

Consani, S., Carbone, C., Salviulo, G., Zorzi, F., Dinelli, E., Botter, R., Nodari, L., Badocco, D., Lucchetti, G., 2016. Effect of temperature on the release and remobilization of ecotoxic elements in AMD colloidal precipitates: the example of the Libiola copper mine, (Italy). Environ. Sci. Pollut. Res. http://dx.doi.org/10.1007/s11356-016-6406-x.

C.N.R. (Consiglio Nazionale delle Ricerche), M.U.R.S.T. (Ministero dell'Università e della Ricerca Scientifica e Tecnologica), 1997M. Atlante Delle Spiagge Italiane: Dinamismo-Tendenza Evolutiva. Opere Umane. S.EL.CA., Firenze 108, Scale 1: 100.000.

Cortecci, G., Boschetti, T., Dinelli, E., Cabella, R., 2008. Sulphur isotopes, trace elements and mineral stability diagrams of waters from the abandoned Fe–Cu mines of Libiola and Vigonzano (northern Apennines, Italy). Water Air Soil Pollut. 192, 85–103. http://dx. doi.org/10.1007/s11270-008-9637-8.

Cox, M.E., Preda, M., 2003. Trace metal distribution and relation to marine sediment mineralogy, gulf of Carpentaria, northern Australia. Baseline. Mar. Pollut. Bull. 46, 1615–1629. http://dx.doi.org/10.1016/j.marpolbul.2003.08.010.

da Silva, E.F., Almeida, S.F.P., Nunes, M.L., Luís, A.T., Borg, F., Hedlund, M., de Sá, C.M., Patinha, C., Teixeira, P., 2009. Heavy metal pollution downstream the abandoned Coval da Mó mine (Portugal) and associated effects on epilithic diatom communities. Sci. Total Environ. 407, 5620–5636. http://dx.doi.org/10.1016/j.scitotenv.2009.06. 047.

DeNicola, D.M., Stapleton, M.G., 2002. Impact of acid mine drainage on benthic communities in streams: the relative roles of

substratum vs. aqueous effects. Environ. Pollut. 119, 303–315 (PII: S0269-7491(02)00106-9).

Di Matteo, A., Milli, M., 2008. Morphological, bathymetric and sedimentological surveys used to assess the coastline defensive measures. Int. J. Environ. Sci. Technol. 5 (3), 415–424.

Dinelli, E., Lucchini, F., Fabbri, M., Cortecci, G., 2001. Metal distribution and environmental problems related to sulfide oxidation in the Libiola copper mine area (Ligurian Apennines, Italy). J. Geochem. Explor. 74, 141–152 (PII: S0375-6742(01)00180-7).

Dinelli, E., Tateo, F., 2002. Different types of fine-grained sediments associated with acid mine drainage in the Libiola Fe-Cu mine area (Ligurian Apennines, Italy). Appl. Geochem. 17, 1081–1092.

Doglioli, A., Griffa, A., Magaldi, M., 2004a. Numerical study of a coastal current on a steep slope in presence of a cape: the case of the Promontorio di Portofino. J. Geophys. Res. 109, C12033. http://dx.doi.org/10.1029/2004JC002422.

Doglioli, A.M., Magaldi, M.G., Vezzulli, L., Tucci, S., 2004b. Development of a numerical model to study the dispersion of wastes coming from a marine fish farm in the Ligurian Sea (western Mediterranean). Aquaculture 231, 215–235. http://dx.doi.org/10. 1016/j.aquaculture.2003.09.030.

Ducci, M., Leoni, L., Marroni, M., Tamponi, M., 1995. Determinazione del grado metamorfico delle Argille a Palombini dell'alta Val Lavagna (Unità Gottero, Appennino Settentrionale). Atti della Società Toscana di Scienze naturali, Memorie Serie A. 102 pp. 39–45 (http://www.stsn.it/serA102/Ducci-Leoni-MarroniTamponi.pdf).

Duran, I., Sanchez-Marin, P., Beiras, R., 2012. Dependence of Cu, Pb and Zn remobilization on physicochemical properties of marine sediments. Mar. Environ. Res. 77, 43–49. http://dx.doi.org/10.1016/j.marenvres.2012.02.001.

Edraki, M., Golding, S.D., Baublys, K.A., Lawrence, M.G., 2005. Hydrochemistry, mineralogy and sulfur isotope geochemistry of acid mine drainage at the Mt. Morgan mine environment, Queensland, Australia. Appl. Geochem. 20, 789–805. http://dx.doi.org/10. 1016/j.apgeochem.2004.11.004.

Gerhardt, A., Janssens de Bisthoven, L., Soares, A.M.V.M., 2004. Macroinvertebrate response to acid mine drainage: community metrics and on-line behavioural toxicity bioassay. Environ. Pollut. 130, 263–274. http://dx.doi.org/10.1016/j.envpol.2003.11.016.

Grosbois, C., Courtin-Nomade, A., Martin, F., Bril, H., 2007. Transportation and evolution of trace element bearing phases in stream sediments in a mining - influenced basin (upper Isle River, France). Appl. Geochem. 22, 2362–2374. http://dx.doi.org/10.1016/j.apgeochem.2007.05.006.

Guerra, G., Pasteris, A., Ponti, M., 2009. Impacts of maintenance channel dredging in a northern Adriatic coastal lagoon. I: effects on sediment properties, contamination and toxicity. Estuarine. Coast. Shelf Sci. 85, 134–142. http://dx.doi.org/10.1016/j.ecss.2009.05.021.

Guigue, J., Mathieu, O., Leveque, J., Denimal, S., Steinmann, M., Milloux, M.J., Grisey, H., 2013. Dynamics of copper and zinc sedimentation in a lagooning system receiving landfill leachate. Waste Manag. 33 (11), 2287–2295 (http://dx.doi.org/10.1016/j.wasman.2013.06.004).

Halter, D., Casiot, C., Heipieper, H.J., Plewniak, F., Marchal, M., Simon, S., Arsène-Ploetze, F., Bertin, P.N., 2012. Surface properties and intracellular speciation revealed an original adaptive mechanism to arsenic in the acid mine drainage bio-indicator Euglena mutabilis. Appl. Microbiol. Biotechnol. 93, 1735–1744. http://dx.doi.org/10.1007/ s00253-011-3493-y.

Harding, J.S., 2005. Impacts of metals and mining on Stream Communities. In: Moore, T.A., Black, A., Centeno, J.A., Harding, J.S., Trumm, D.A. (Eds.), Metal Contaminants in New Zealand. Resolutionz press, Christchurch, NZ, pp. 343–357.

Johnson, D.B., Hallberg, K.B., 2005. Acid mine drainage remediation options: a review. Sci. Total Environ. 338, 3–14. http://dx.doi.org/10.1016/j.scitotenv.2004.09.002.

Kimball, B.A., Callender, E., Axtmann, E.V., 1995. Effects of colloids on metal transport in a river receiving acid mine drainage, upper Arkansas River, Colorado, U.S.A. Appl. Geochem. 10, 285–306.

Lin, Z., Puls, R.W., 2000. Adsorption, desorption and oxidation of arsenic affected by clay minerals and aging process. Environ. Geol. 39, 753–759.

Luís, A.T., Teixeira, P., Almeida, S.F.P., Ector, L., Matos, J.X., Ferreira da Silva, E.A., 2009. Impact of acid mine drainage (AMD) on water quality, stream sediments and periphytic diatom communities in the surrounding streams of Aljustrel mining area (Portugal). Water Air Soil Pollut. 200, 147–167. http://dx.doi.org/10.1007/s11270-008-9900-z.

Marescotti, P., Carbone, C., De Capitani, L., Grieco, G., Lucchetti, G., Servida, D., 2008. Mineralogical and geochemical characterisation of open-air tailing and waste-rock dumps from the Libiola Fe-Cu sulphide mine (eastern Liguria, Italy). Environ. Geol. 53, 1613–1626. http://dx.doi.org/10.1007/s00254-007-0769-8.

Marini, L., Saldi, G., Cipolli, F., Ottonello, G., Zuccolini, M.V., 2003. Geochemistry of water discharges from the Libiola mine, Italy. Geochem. J. 37 (2), 199–216.

Martins, R., Azevedo, M.R., Mamede, R., Sousa, B., Freitas, R., Rocha, F., Quintino, V., Rodrigues, A.M., 2012. Sedimentary and geochemical characterization and provenance of the Portuguese continental shelf soft-bottom sediments. J. Mar. Syst. 91, 41–52. http://dx.doi.org/10.1016/j.jmarsys.2011.09.011.

Matlock, M.M., Howerton, B.S., Atwood, D.A., 2002. Chemical precipitation of heavy metals from acid mine drainage. Water Res. 36, 4757–4764 (PII: S0043-1354(02)00149-5).

Millot, C., Taupier-Letage, I., 2005. Circulation in the Mediterranean Sea. The Handbook of Environmental Chemistry. 5, Part K pp. 29–66. http://dx.doi.org/10.1007/b107143.

Morillo, J., Usero, J., Gracia, I., 2004. Heavy metal distribution in marine sediments from the southwest coast of Spain. Chemosphere 55, 431–442. http://dx.doi.org/10.1016/j.chemosphere.2003.10.047.

Nicolau, R., Galera-Cunha, A., Lucas, Y., 2006. Transfer of nutrients and labile metals from the continent to the sea by a small Mediterranean river. Chemosphere 63, 469–476. http://dx.doi.org/10.1016/j.chemosphere.2005.08.025.

Nieto, J.M., Sarmiento, A.M., Olìas, M., Canovas, C.R., Riba, I., Kalman, J., Delvalls, T.A., 2007. Acid mine drainage pollution in the Tinto and Odiel rivers (Iberian Pyrite Belt, SW Spain) and bioavailability of the transported metals to the Huelva estuary.

Environ. Int. 33, 445–455. http://dx.doi.org/10.1016/j.envint.2006.11.010.

Passarelli, P., 2001. Comuni d'Italia - Liguria. Istituto enciclopedico italiano. 9 (287 pp. ISBN: 8887983119).

Preda, M., Cox, M.E., 2002. Trace metal occurrence and distribution in sediments and mangroves, Pumicestone region, Southeast Queensland, Australia. Environ. Int. 28, 433–449 (PII: S0160-4120(02)00074-0).

di Genova, P., 2009. Piano di Bacino, Stralcio sul bilancio idrico. Il bacino del Torrente Gromolo (124 pp. http://cartogis.cittametropolitana.genova.it/cartogis/pdb/bilancio_idrico/bilancio_idrico/documenti/RelazioneGromolo.pdf).

Romano, E., Bergamin, L., Finoia, M.G., Carboni, M.G., Ausili, A., Gabellini, M., 2008. Industrial pollution at Bagnoli (Naples, Italy): benthic foraminifera as a tool in integrated programs of environmental characterisation. Mar. Pollut. Bull. 56, 439–457. http:// dx.doi.org/10.1016/j.marpolbul.2007.11.003.

Salomons, W., Forstner, U., 1984. Metals in the Hydrocycle. Springer, Berlin, Germany.

Schintu, M., Buosi, C., Galgani, F., Marrucci, A., Marras, B., Ibba, A., Cherchi, A., 2015. Interpretation of coastal sediment quality based on trace metal and PAH analysis, benthic foraminifera, and toxicity tests (Sardinia, Western Mediterranean). Mar. Pollut. Bull. 94, 72–83. http://dx.doi.org/10.1016/j.marpolbul.2015.03.007.

Shaari, H., Azmi, S.N.H.M., Sultan, K., Bidai, J., Yuzwan, M., 2015. Spatial distribution of selected heavy metals in surface sediments of the EEZ of the east coast of Peninsular Malaysia. Int. J. Oceanol., 618074 http://dx.doi.org/10.1155/2015/618074 (10 pages).

Sheoran, A.S., Sheoran, V., 2006. Heavy metal removal mechanism of acid mine drainage in wetlands: a critical review. Miner. Eng. 19, 105–116. http://dx.doi.org/10.1016/j. mineng.2005.08.006.

Shoham-Frider, E., Shelef, G., Kress, N., 2007. Mercury speciation in sediments at a municipal sewage sludge marine disposal site. Mar. Environ. Res. 64, 601–615. http://dx.doi. org/10.1016/j.marenvres.2007.06.003.

Van Meirvenne, M., Goovaerts, P., 2001. Evaluating the probability of exceeding a sitespecific soil cadmium contamination threshold. Geoderma 102, 75–100 (PII: S00167061(00)00105-1).

Villaescusa-Celaya, J.A., Gutiérrez-Galindo, E.A., Flores-Muñoz, G., 2000. Heavy metals in the fine fraction of coastal sediments from Baja California (Mexico) and California (USA). Environ. Pollut. 108, 453–462 (PII: S0269-7491(99)00222-5).

Wainipee, W., Cuadros, J., Sephton, M.A., Unsworth, C., Gill, M.G., Strekopytov, S., Weiss, D.J., 2013. The effects of oil on As(V) adsorption on illite, kaolinite, montmorillonite and chlorite. Geochim. Cosmochim. Acta 121, 487–502.

Yuan, C., Shi, J., He, B., Liu, J., Liang, L., Jiang, G., 2004. Speciation of heavy metals in marine sediments from the East China Sea by ICP-MS with sequential extraction. Environ. Int. 30, 769–783.

Zaccarini, F., Garuti, G., 2008. Mineralogy and chemical composition of VMS deposits of northern Apennine ophiolites, Italy: evidence for the influence of country rock type on ore composition. Mineral. Petrol. 94, 61–83. http://dx.doi.org/10.1007/s00710008-0010-9.

Zhu, H., Yuan, X., Zeng, G., Jiang, M., Liang, J., Zhang, C., Yin, J., Huang, H., Liu, Z., Jiang, H., 2012. Ecological risk assessment of heavy metals in sediments of Xiawan port based on modified potential ecological risk index. Trans. Nonferrous Metals Soc. China 22, 1470–1477. http://dx.doi.org/10.1016/S1003-6326(11)61343-5.